Yamaguchi and Furuya
Earth, Planets and Space (2024) 76:1
https://doi.org/10.1186/s40623-023-01944-y

Earth, Planets and Space

EXPRESS LETTER Open Access

Can we explain the post-2015 absence of the Chandler wobble?

Ryuji Yamaguchi[1*] and Masato Furuya[2,3]

Abstract

Recent polar motion data do not show a 6-year beat and indicate the absence of the Chandler wobble (CW), whereas we could observe the 6-year beat even in the 1920-40 s when the CW amplitude was known to be smallest. As a free mode, the CW needs excitation one or more sources that were debated decades ago but are now attributed to the atmosphere, ocean, and possibly land water. Here, we show that the anomaly started in 2015, after which two independent estimates of the atmospheric CW excitation became persistently smaller than before. However, the estimates of the oceanic and land–water contributions are too large, suggesting improved estimates are needed. Taking advantage of the recent CW anomaly, we show that the quality factor of CW is not as high as 100 as previously preferred. Although the CW excitation processes have been assumed random, a termination of near-resonant processes would rather be consistent with the present findings.

Keywords Chandler wobble, Excitation process, Quality factor, Atmospheric angular momentum, 6-year beat

Graphical Abstract

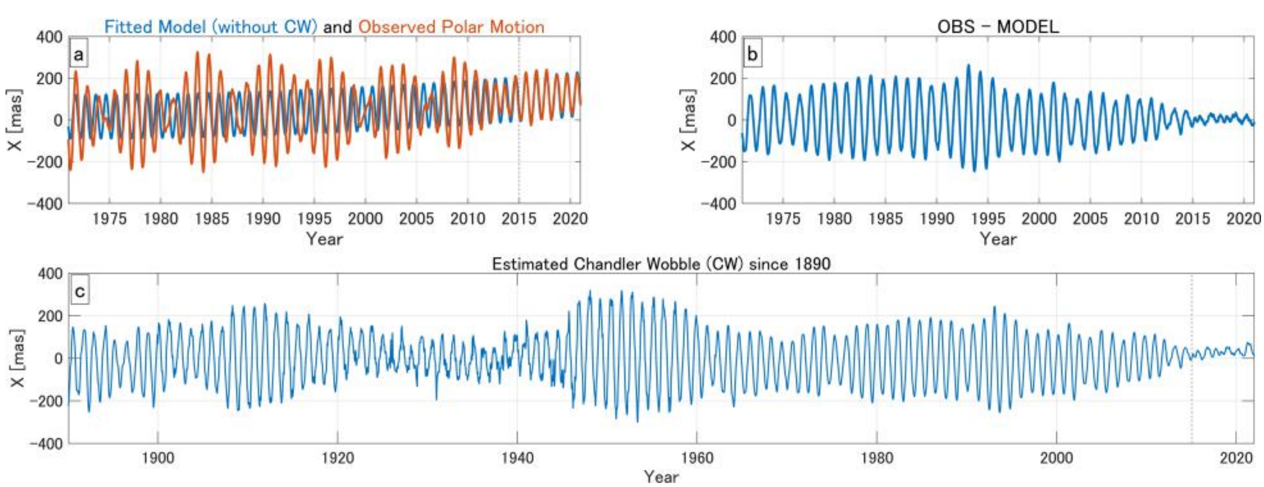

*Correspondence:
Ryuji Yamaguchi
jiktm@eis.hokudai.ac.jp
Full list of author information is available at the end of the article

Introduction

The Chandler wobble (CW) and annual wobble (AW) are two dominant near-circular components in the Earth's polar motion, a long period (> 1 day) motion of the Earth's spin axis relative to the rotating solid Earth (Munk and MacDonald 1960; Gross 2015). Because of their comparable amplitude and the 1.2-year period of the CW (*P*), the polar motion time series has been exhibiting a 6-year beat for over a century besides the secular drift of the mean pole toward the 79°W direction (Fig. 1a and Additional file 1: S1a). While the AW is a forced motion by seasonal angular momentum exchanges between surface fluids and the solid Earth around the equatorial axes, the CW, as a free oscillatory mode, requires one or more excitation sources that were elusive until the early 2000s (e.g., Gross 2015). While earthquakes were once considered as candidates but denied quantitatively (e.g., Dahlen 1973), it is now widely believed that the atmosphere, ocean, and possibly continental water are the excitation sources (e.g., Furuya et al. 1996; Aoyama and Naito 2001; Aoyama et al. 2003; Brzeziński and Nastula 2002; Gross 2000; Seitz and Schmidt 2005). However, there is still a threefold variation in the estimated quality factor (*Q*) of the CW from 50 to 179 that controls both its damping time and the required excitation power (e.g., Wilson and Vicente 1990; Furuya and Chao 1996; Seitz and Schmidt 2005; Seitz et al. 2012; Nastula and Gross 2015), indicating our incomplete understanding of the excitation sources and processes. Moreover, *Q* of the CW is a unique parameter that can constrain the frequency-dependent deformation response of the solid Earth, particularly the lower mantle (Smith and Dahlen 1981; Benjamin et al. 2006), and bridge the order-of-magnitude gap between the seismic, semi-diurnal and long-period (18.6 years) frequencies (Benjamin et al. 2006).

Recent polar motion data lack the 6-year beat that was previously clearly observed (Fig. 1a). While the CW amplitude is known to have been smallest in the 1920-40 s (e.g., Vondrák and Ron 2005; Malkin and Miller 2010), we could readily recognize the presence of the 6-year beat even in the 1920-40 s; we consider only the data after 1900 because the observation errors before 1900 are greater than 50 mas (International Earth Rotation and Reference System Service (IERS) website). The mas stands for milliarcsecond in angle, where one mas is equivalent to ~ 3 cm on the Earth surface. We show below by simple least squares approach that the recent CW is much smaller than before, implying that the CW is essentially unexcited in recent years (Fig. 1b, c), while Zotov et al. (2022) also pointed out the recent zero CW through singular spectrum analysis (SSA). We are also informed that the CW signal in super-conducting gravimeter data at Syowa Station, Antarctica, has been weakened since several years ago (Personal communications with Yuichi Aoyama, Unpublished data).

Although the CW must have been continually excited by the Earth's surface fluids for over a century, how can we interpret the recent un-excitation? Now that high-precision space geodetic data are available and that global Earth system modeling allows us to compute higher-quality atmospheric, oceanic, and hydrological angular momentum (AAM, OAM, and HAM) data sets as the

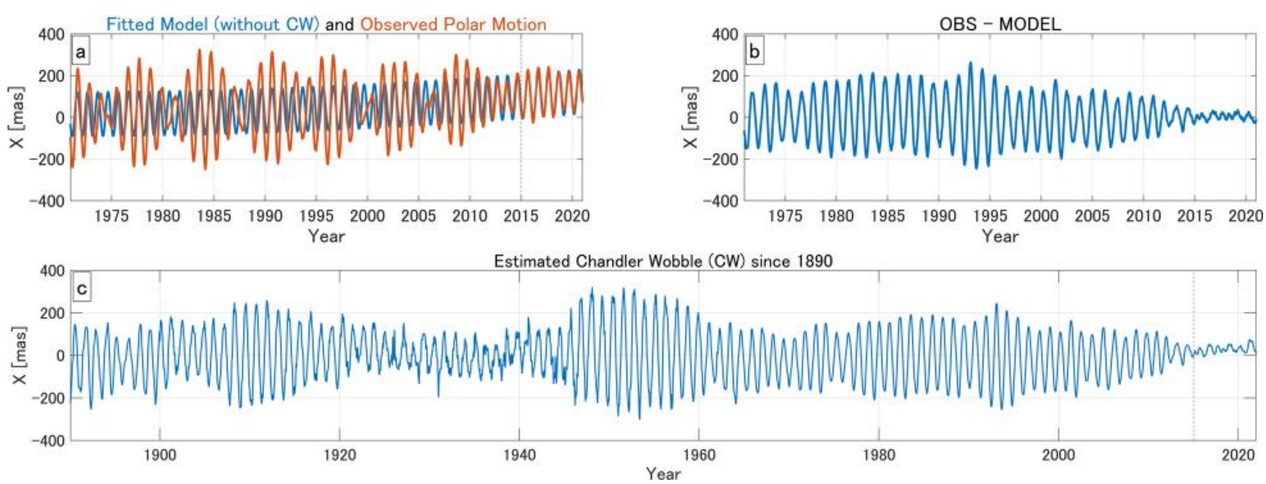

Fig. 1 The polar motion time-series. (**a**) The X-component of the polar motion data, EOP 14 C04, since 1976 (red) and the polar motion model (blue) by fitting the data from 2015 to 2021 with only the AW and long-term polar drift period and extending back to 1971. (**b**) Estimated CW since 1971 by taking a difference between the two time-series in (**a**). Note that we do not assume any Chandler period (*P*) and *Q* of the CW. **c** Similar to **b** but extended time-series back to 1890, using the polar motion data, EOP C01 IAU1980. The Y-components are shown in Additional file 1: Figure S1.

estimates of excitation, we examine if the present Earth system modeling data can explain the anomaly and discuss why the CW is not as extensively excited as before. Understanding the excitation and un-excitation processes of the CW will also have implications for polar motion prediction; the presence of freely damped CW, if any, will make the polar motion prediction much simpler because the CW dominates over the "rapid polar motion" with timescales between 2 weeks to several months (Eubanks et al. 1989). In addition, even if the geophysical excitation data are not accurate enough, we can take advantage of the recent CW anomaly to more tightly constrain the upper bound of Q of the CW.

Data and methods

Polar motion data

We use the earth orientation parameter (EOP) data, EOP 14 C04 for the recent decades and EOP C01 going back to 1846 (Bizouard et al. 2019). Because the AW does not change its phase by definition and its amplitude is nearly constant (Gross 2015), we can fit the polar motion data from 2015 to 2021 with a simple two-component model consisting of only the AW and secular drift (Fig. 1); fitting the seasonal signals with constant-amplitude sinusoids is a conventional approach to studying the CW excitation (e.g., Gross 2000), and we approximate the secular drift with a second-order polynomial. Subtracting the two-component time series from the original data with an extension to 1971, we observe that the CW started to be weaker in 2005 and became insignificant in 2015 (Fig. 1b). The post-2015 smaller-amplitude signals in Fig. 1b will indicate either the so-called rapid polar motion (Eubanks et al. 1988) and/or the modulated amplitude in the AW and have to be distinguished from the previously observed CW; if the CW were present as previously even after 2015, we should have observed a 6-year beat in recent years as well. Extending the two-component model to 1890, we could reproduce and confirm the smaller CW in 1920–40 (Fig. 1c). The post-2015 small amplitude in Fig. 1b might well include some CW signals but no such small amplitude CW had been observed before. Thus, for simplicity, we refer to the post-2015 CW as the "absence"; even though the post-2015 CW amplitude is not exactly zero, our conclusions below do not change.

Polar motion theory and excitation functions

Theoretically, the Earth's wobble, $\widetilde{p}(t) \equiv x(t) - iy(t)$, is considered to be generated through a convolution of an impulse response function, $e^{i\widetilde{\sigma}_{cw}t}$ with excitation sources, $\widetilde{\chi}(t)$:

$$\tilde{p}(t) = \tilde{p}_0 e^{i\tilde{\sigma}_{cw}(t-t_0)} - i\tilde{\sigma}_{cw}\int_{t_0}^{t} e^{i\tilde{\sigma}_{cw}(t-\tau)}\tilde{\chi}(\tau)d\tau \quad (1)$$

The first term indicates a freely damping term due to the cumulative excitations by the time $t = t_0$. The second term represents the wobble excited after $t = t_0$ (Munk and MacDonald 1960); the complex form for the pole position and excitation allows us to analyze the 2-D motion with 1-D data. Here, $x(t)$ and $y(t)$ indicate the location of the North Pole along the Greenwich meridian and the 90° West Longitude, respectively, and $\widetilde{\sigma}_{cw} \equiv 2\pi/P(1 + i/2Q)$ is the complex characteristic frequency defined by the Chandler period and Q. Conventional approach to examine the polar motion excitation is first to perform deconvolution of the observed data, $\widetilde{p}(t)$ into "geodetic" excitation, $\widetilde{\chi}_{geod}(t)$ with an assumed pair of P and Q (Wilson 1985). We can compute "geophysical" excitation, $\widetilde{\chi}_{geoph}(t)$ independently from $\widetilde{\chi}_{geod}(t)$, using global Earth system modeling and assimilation data that became available as AAM in the early 1980s (Barnes et al. 1983) and OAM in the late 1990s (Ponte et al. 1998). The AAM and OAM include both the mass (moment of inertia tensor) and motion (relative angular momentum) terms, where surface air and ocean bottom pressure changes contribute to the mass term, and atmospheric wind and ocean current contribute to the motion term. We assumed that the ocean surface responds to reduce variation of the air pressure, which is called an "inverted barometer". Nowadays, land water hydrological effect is also estimated as HAM based on the Land Surface Discharge Model (Dill 2008). After considering the effect of elastic response and core-mantle decoupling (e.g., Gross 2015), we can compare the "geodetic" excitation, $\widetilde{\chi}_{geod}(t)$ with "geophysical" excitations, $\widetilde{\chi}_{geoph}(t)$. Table 1 lists the geophysical excitation data sets in this study and Additional file 1: Figure S2 is the flowchart to calculate $\widetilde{p}_{geoph}$ and $\widetilde{p}_{geod}$.

Analysis approach in this study

Analysis approach in this study is to compare in the wobble domain. Performing the convolution with any geophysical excitations on the assumption of P and Q, we may compare the geodetic wobble, $\widetilde{p}_{geod}(t)$, with the geophysical wobble, $\widetilde{p}_{geoph}(t)$. For the analysis of the CW excitation sources, we think that the wobble domain approach performs better than the excitation domain approach because we can amplify any small excitation signals around the resonant frequency that essentially contribute to excite the CW (Furuya et al. 1997). Although the same conclusion should be drawn in theory, we are led to compare small amplitude signals in both geodetic and geophysical data in the excitation

Table 1 Geophysical excitation data used in this study

Data	Components	Data provided from	Data term
ESMGFZ (Dobslaw et al. 2010)	ECMWF AAM (atmospheric angular momentum)	Deutsches GeoForschngsZentrum (GFZ)	1976 ~ 2021
	MPIOM OAM (oceanic angular momentum)		
	LSDM HAM (hydrospheric angular momentum)		
NCEP + ECCO (Gross et al. 2003)	NCEP AAM	Paris Observatory	1962 ~ 2021 (A)
	ECCO OAM		1962 ~ 2018 (O)
JRA-55 AAM (This Study)	JRA-55 AAM	Original JRA-55 data by Japan Meteorological Agency (JMA) (Kobayashi et al. 2015)	1960 ~ 2021

domain. Moreover, performing the comparison in frequency domain as many previous studies (e.g., Furuya et al. 1996; Gross 2000; Aoyama and Naito 2001), the frequency resolution is seriously limited by the available data length. Nonetheless, most previous studies have circumvented the wobble domain approach because the first term in Eq. 1 represents a free damping that generates a non-zero CW amplitude even without any excitations afterward (Chao 1985). However, if we start the convolution with zero initial value, we can more directly evaluate if and how much the candidate sources can excite and maintain the CW. Chao (1985) did not mention another caveat for the wobble domain analysis. Namely, we must take out the seasonal signals before convolution (integration) because, even if the integration starts from zero initial value, a sudden start of large seasonal forcing will generate a transient CW that is not present in actual data. Such a transient CW is canceled by a damped CW excited by seasonal forcing; seasonal forcing eventually generates only seasonal wobble in a linear dynamical system. The geodetic CW can thus be derived by re-convolving (re-integrating) the deconvolved non-seasonal geodetic excitation with the same P and Q (Furuya et al. 1997). The drawback in the wobble domain approach is that there arises the same issue as the "non-zero" initial value when the integration time is extended. However, it also depends on the time scale of the damping of CW, i.e., prescribed Q; precision estimation of CW's Q is, therefore, important.

Results

Sensitivity of the results to *P* and *Q*

To demonstrate the sensitivity of $\widetilde{p}_{geod}(t)$ and $\widetilde{p}_{geoph}(t)$ to assumed P and Q, Fig. 2 shows five cases of the x component from $\widetilde{p}_{geod}(t)$ and $\widetilde{p}_{geoph}(t)$ with different pairs of P and Q; essentially the same result is observed in the y component (Additional file 1: Figure S3). To compute $\widetilde{p}_{geoph}(t)$ by $\widetilde{\chi}_{geoph}(t)$ in Fig. 2, we summed up the AAM, OAM, and HAM provided by the Earth System Modeling Group at GeoForschngsZentrum (ESMGFZ) in Table 1 that computed the total angular momentum changes within the Earth's surface fluid system most comprehensively. Notably, $\widetilde{p}_{geod}(t)$ indeed show a much smaller amplitude after 2015, whereas the amplitude and phase also depend on the pair of P and Q. Moreover, we observe that $\widetilde{p}_{geoph}(t)$ varies sensitively to the assumed pair of P and Q, and thus we can tightly constrain optimum P and Q by matching $\widetilde{p}_{geod}(t)$ and $\widetilde{p}_{geoph}(t)$ (Fig. 2). The discrepancies between $\widetilde{p}_{geod}(t)$ and $\widetilde{p}_{geoph}(t)$ suggest either that the pair of P and Q is inadequately assumed or that any of $\widetilde{\chi}_{geoph}(t)$ still incompletely captures the real geophysical excitations or both. However, based on the currently available data, we may claim that optimum P is 432 days and that Q is unlikely to be as high as 100, judging from Fig. 2e. Although the smallest Q of 25 better matches the post-2015 smaller signal (Fig. 2b), there are significant discrepancies from the 1980s to the early 2000s (Fig. 2d).

Can the available geophysical data reproduce the recent CW?

To account for the recent absence of the CW, we may conceive various scenarios in each of the AAM, OAM, and HAM contributions, respectively. For instance, all three contributions since 2015 may be equally smaller than before. Or lternatively, the total sum of the three contributions could happen to cancel each other and become nearly zero, whereas each of them might have substantial amplitude even after 2015. We examine in the wobble domain the contributions from three AAM (Fig. 3a–c), two OAM (Fig. 3d, e) originally driven by the same atmospheric data in Fig. 3a, b, and one HAM (Fig. 3f) estimated from the Earth system modeling along with Fig. 3a, d (Dobslaw et al. 2010). We fixed P and Q with 432 days and 50, derived from the results in Fig. 2. Although the AAM alone is not enough to explain the CW from the 1970s to 1990s (Fig. 3a–c), we observe that the three AAMs are roughly consistent with each other in terms of both amplitude and phase of the computed CW,

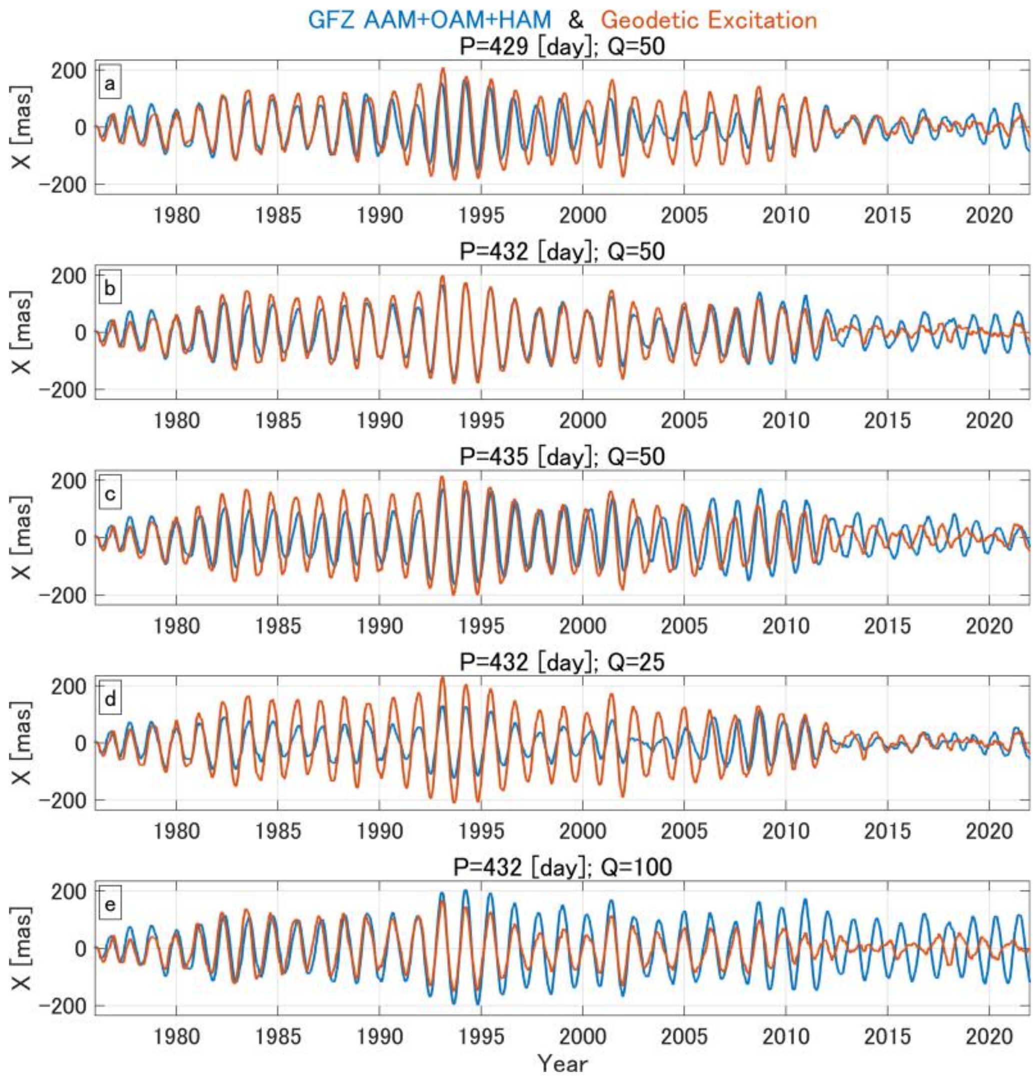

Fig. 2 Comparisons of the estimated geodetic and geophysical CW as a function of *P* and *Q* (X-component). **a** *P* = 429 days, *Q* = 50, **b** *P* = 432 days, *Q* = 50, **c** *P* = 435 days, *Q* = 50, **d** *P* = 432 days, *Q* = 25, **e** *P* = 432 days, *Q* = 100. See Additional file 1: Figures S3 and Additional file 1: S4 for Y-component and other choices of *P* and *Q*, respectively.

and two of them further indicate persistently smaller amplitude since 2015 (Fig. 3a, c).

On the other hand, the two OAMs are not as consistent as the three AAMs and do not significantly change the amplitude even after 2015 (Fig. 3d, e). Moreover, the HAM generates rather a greater CW in the recent period (Fig. 3f) and seems responsible for the significant discrepancies after 2015 in Fig. 2b. We thus recognize that the available OAM and HAM may still include some errors and biases (Fig. 3d–f), whereas the two AAMs (Fig. 3a–c) are almost in perfect agreement. It is uncertain if both the OAM and HAM have become smaller or if they have been canceling each other since 2015.

A simple approach to constrain the upper bound of Q

We can exploit the recent non-excitation of the CW to more simply constrain the upper bound of *Q* without using any geophysical data. While those geodetic CW in Figs. 2 and 3 are derived by re-integrating non-seasonal $\widetilde{\chi}_{geod}(t)$ with prescribed *P* and *Q*, we should note that the CW in Figs. 1b, c were derived without any assumptions of *P* and *Q*. Denoting the geodetic CW in Figs. 2 and 3 as the CW_{GEOD} and the latter in Fig. 1 as the CW_{OBS}, Fig. 4 shows a comparison of a series of CW_{GEOD} with CW_{OBS}. Because the first term of Eq. 1 is excluded in the CW_{GEOD}, causing the disagreement during the early- to mid-period, we should focus on to what extent the CW_{GEOD} and the CW_{OBS} match during the recent period.

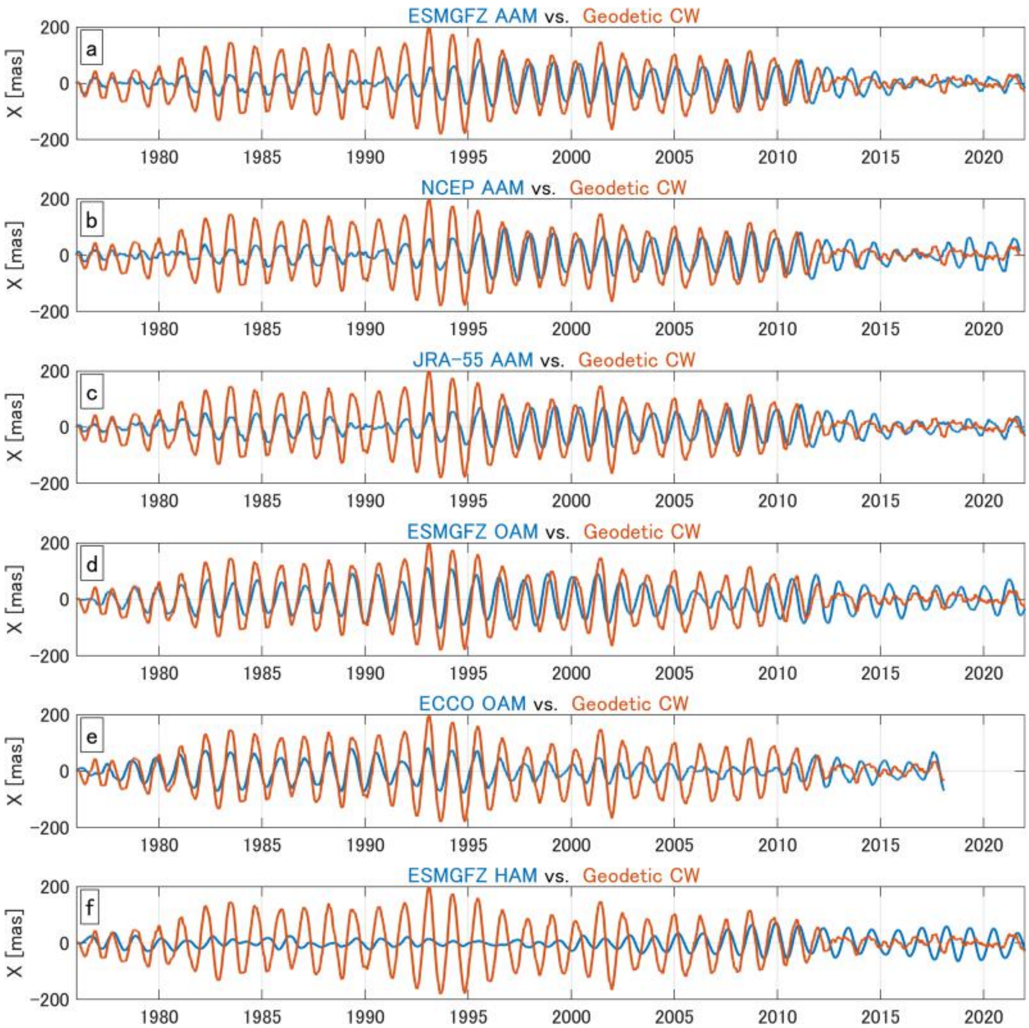

Fig. 3 Contributions to the estimated CW from each geophysical excitation data (X-component). Case with $P = 432$ days and $Q = 50$ **a** ESMGFZ AAM, **b** NCEP AAM, **c** JRA-55 AAM, **d** ESMGFZ OAM, **e** NCEP/ECCO OAM, **f** ESMGFZ HAM.

It turns out again that larger Q (>100) is unlikely and should be below 50, which we already observed in Fig. 2e. Still, it should be noted that we can conclude as such without using any geophysical data because the CW has not been excited during the recent period.

Changing prescribed P, we have also repeated those computations and examined the variance reduction between the CW_{GEOD} and CW_{OBS} since 2015. It turns out that this approach is insensitive to P and does not tell optimum P (Additional file 1: Figure S5) because the deconvolution and the following convolution do not affect the amplitude of the estimated CW as long as P is consistently prescribed both in the deconvolution and in the re-convolution. We confirm that Q is unlikely to be greater than 100. Although lower Q as much as 25 also gives good agreement, we have shown in Fig. 2d that $Q \sim 25$ is too low to account for the CW in the 1980–2000s. Because the CW is indeed not excited recently, we would be led to lower Q. We need geophysical excitation data to constrain the lower bound of Q.

Discussions

Implications of the recent CW anomaly for excitation processes and global warming

Figures 1 and 2 indicate that the CW started to become smaller in ~ 2005 and almost disappeared in 2015. We may recall the shift in the direction of the secular polar drift to the east since ~ 2005, which was attributed to the rapid ice melting in Greenland (Chen et al. 2013). However, the effect of abrupt ice melting will have more impact in the lower frequency than around the Chandler frequency and thus is not directly related to the CW absence. Nonetheless, we consider that both anomalies in the secular drift and the CW would be more or less

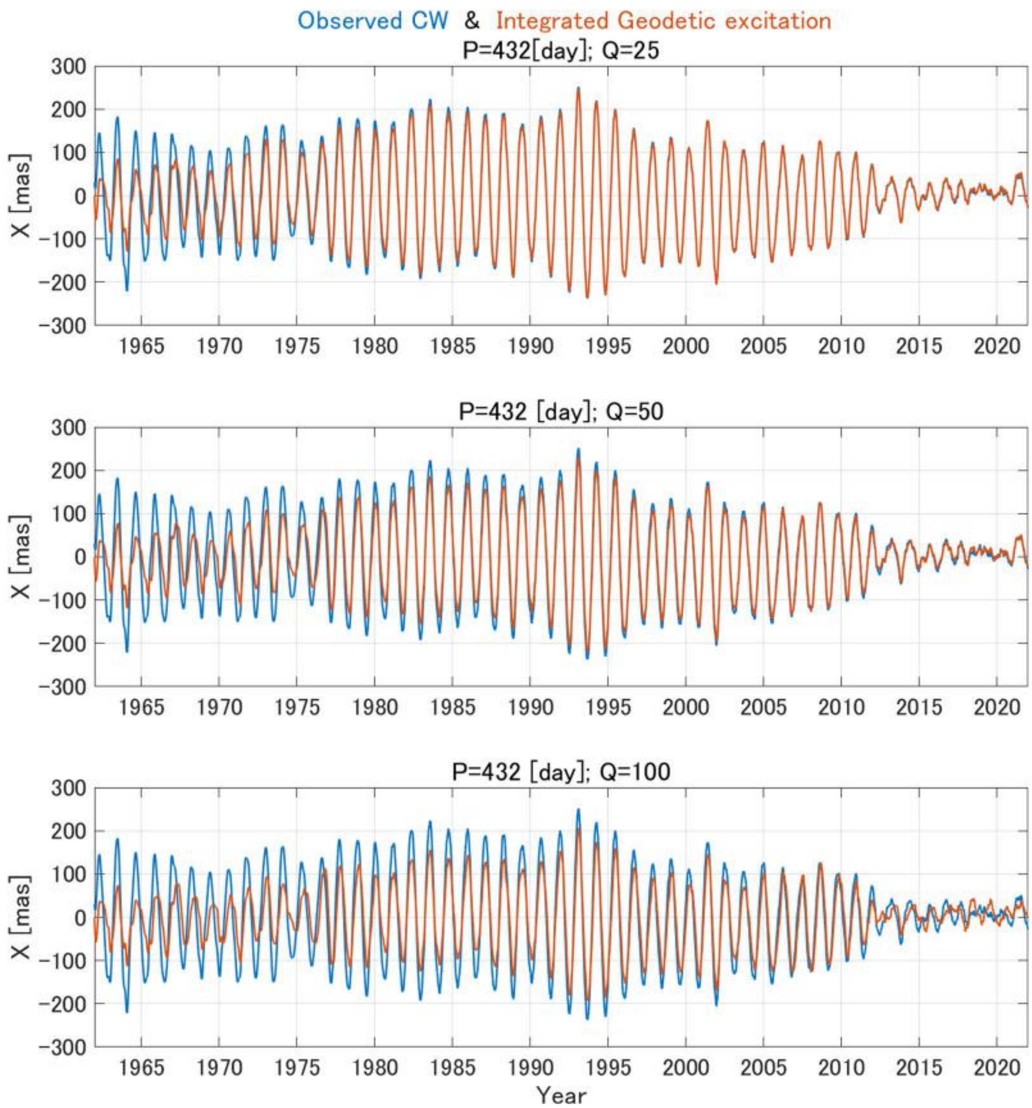

Fig. 4 Comparisons of the "geodetic CW" (red) with the "observed CW" (blue) derived with (red) and without (blue) assuming *P* and *Q* (X-component). The geodetic and observed CW are the same as those in Figs. 2 and 1b, respectively.

associated with the recent global warming trend. It is not straightforward, however, to relate the trend to the CW absence.

Why is the CW not excited since 2015? Regarding the excitation processes of the CW, it is still an open question whether they are random or nearly resonant. Numerous previous studies on the CW excitations have assumed (or believed) the Gaussian random process (e.g., Okubo 1982; Chao 1985; Chao and Chung 2012), and the random excitation model will regard the post-2015 CW anomaly as "simply fortuitous by chance" (Chao and Chung 2012). However, if we take a simple analogy with the classical thermal-noise model, global warming would increase the noise level and amplify the CW, which conflicts with the observation. On the other hand, several earlier studies instead suggested a near-resonant excitation, in which the CW has been maintained by quasi-periodic excitation with a characteristic period of ~ 14 months in the atmosphere (Furuya et al. 1996; Plag 1997; Aoyama and Naito 2001; Aoyama et al. 2003) and the ocean (Plag 1997); note that those studies do not claim that the polar motion follows a non-linear dynamical system. The CW absence may be interpreted as an abrupt termination of such processes. The recent persistently smaller AAM contributions in Fig. 3a–c are for the first time in decades and seem to be in accord with this model; the three AAM time-series data are nearly identical to each other (Additional file 1: Figure S6), and the deviation of Fig. 3b would be due to the small but different spectral content around the Chandler frequency. Although the periodicity of ~ 14 months is unclear in Fig. 3a–c, even a small amplitude is enough if it is close to *P*, and its amplitude needs not to be constant, either. Moreover, any near-resonant excitation sources, if any and not limited to AAM, can more easily excite the CW even with lower *Q*.

Concerning the recent smaller atmospheric excitation, we note the disruption of the equatorial quasi-biennial oscillation (QBO) in the 2015/2016 winter (Osprey et al. 2016; Newman et al. 2016) and 2019/2020 winter (Antsey et al. 2021), which have never been observed before, either. As the QBO itself is zonal wind oscillation in the tropics with a mean period of 28 months (Baldwin et al. 2001), it only affects the length-of-day change (Chao 1989), and no corresponding periodicity should be expected in the polar motion. However, the atmospheric circulation system associated with the QBO would not be strictly longitudinally symmetric and can affect the equatorial angular momentum budget that also includes meridional winds; the role of meridional momentum transport is indeed pointed out for the recent QBO disruptions (Osprey et al. 2016; Newman et al. 2016; Antsey et al. 2021). Although the dynamical relations between the QBO and the ~ 14 months oscillations in AAM are unclear now, the recent smaller AAM in Fig. 3a–c is possibly associated with the QBO disruptions. Similar QBO disruptions are predicted in several climate models under warming scenarios (Osprey et al. 2016; Antsey et al. 2021). The meteorological origins of the recent smaller AAM contributions in Fig. 3 are uncertain and need further examination in detail.

Summary

Although polar motion data have exhibited a 6-year beat for over a century, it has been absent since 2015, indicating that the CW was not excited. We examined if the available estimates of atmospheric, oceanic, and land–water excitation could reproduce the anomaly. It turned out that atmospheric CW excitation became persistently smaller than before but that the estimates of those oceanic and land–water contributions were not consistent enough, suggesting further room to improve their accuracies. Taking advantage of the recent CW anomaly, we show that the quality factor of CW is not as high as the previously preferred 100, indicating that the required CW excitation power is higher than expected before. Although the CW excitation processes have been widely assumed to be random, the recent absence might indicate a termination of more coherent excitation processes.

Abbreviations

AAM	Atmosphere Angular Momentum
AW	Annual Wobble
CW	Chandler Wobble
ECCO	Estimating the Circulation and Climate of the Ocean
ECMWF	European Center Medium-range Weather Forecast
ESMGFZ	Earth System Modeling Group at GeoForschngsZentrum
EOP	Earth Orientation Parameter
HAM	Hydrological Angular Momentum
IERS	International Earth Rotation and Reference Systems Service
JMA	Japan Meteorological Agency
JRA-55	The Japanese 55-year Reanalysis
LSDM	Land Surface Discharge Model
mas	Milliarcseconds
MPIOM	Max-Plank Institute Ocean Model
NCEP	National Centers of Environmental Prediction
OAM	Oceanic Angular Momentum
QBO	Quasi-Biennial Oscillation
SSA	Singular Spectrum Analysis

Supplementary Information

The online version contains supplementary material available at https://doi.org/10.1186/s40623-023-01944-y.

Additional file 1: Figure S1. (a) The Y-component of the polar motion data, EOP 14 C04, since 1971 (red) and the polar motion model (blue) derived by fitting the data from 2015 to 2021 with only AW and long-term polar drift period and extending back to 1971. The *mas* stands for milliarcseconds, where one *mas* is equivalent to ~3cm on the Earth's surface. (b) Estimated CW since 1971 by taking a difference between the two timeseries in (a). Note that we do not assume any *P* and *Q* of the CW. (c) Similar to (b) but extended time-series back to 1890, using the polar motion data, EOP C01 IAU2000. The X-component is shown in Fig. 1. **Figure S2**. A flowchart of the procedure to calculate $\widetilde{p}_{geoph}(t)$ and $\widetilde{p}_{geod}(t)$. We integrated the geophysical excitation ($\widetilde{\chi}_{geoph}$) after removing seasonal components to estimated CW ($\widetilde{p}_{geoph}$). Then, we set the initial value to be zero. To calculate $\widetilde{p}_{geod}$, we followed the same procedure for $\widetilde{\chi}_{geoph}$, which was calculated by deconvoluting the observed polar motion data. **Figure S3**. Comparisons of the estimated geodetic and geophysical CW as a function of the *P* and *Q* (Y-component). (a) *P*=429 days, *Q*=50, (b) *P*=432 days, *Q*=50, (c) *P*=435 days, *Q*=50, (d) *P*=432 days, *Q*=25, (e) *P*=432 days, *Q*=100. See Fig. S3 for other choices of *P* and *Q*. The X-component is shown in Fig. 2. **Figure S4.** Comparisons of the estimated geodetic and geophysical CW as a function of the assumed *P* and *Q* not shown in Fig 2. (a and b) X- and Y-component for *P*=429 days, *Q*=25, (c and d) The case of *P*=429 days, *Q*=100, (e and f) The case of *P*=435 days, *Q*=25, (g and h) The case of *P*=435 days, *Q*=100. **Figure S5.** Variance reduction (VR) between CW_{OBS} and CW_{GEOD} as a function of prescribed *P* and *Q*. The maximum VR is one. **Figure S6**. Comparisons of ECMWF (blue), NCEP (red), and JRA-55 AAM (yellow) in 2000. The annual component and the quadratic long-term motion are removed from all data. The NCEP AAM data were shifted by three days from the original data available from Paris observatory.

Acknowledgements

We acknowledge two anonymous reviewers, whose comments improved the original manuscript. We thank Kosuke Heki for his comments on the earlier manuscript and Yuichi Aoyama for discussion on the AAM computation and superconducting gravimeter data, which were helpful to improve the manuscript. This work was supported by JST, the establishment of university fellowships towards the creation of science technology innovation, Grant Number JPMJFS2101. The author YR received the Seto Prize of the Geodetic Society of Japan and this study was supported by the award.

Author contributions

YR analyzed the data and drafted the manuscript. MF conceptualized, supervised, and approved the final draft.

Funding
Yamaguchi Ryuji is supported by the Ambitious Doctoral Fellowship, Hokkaido University, which is funded by JST, the establishment of university fellowships towards the creation of science technology innovation, Grant Number JPMJFS2101.

Availability of data and materials
The polar motion data, EOP C01 and EOP 14 C04, are available from the IERS, https://www.iers.org/IERS/EN/DataProducts/EarthOrientationData/eop.html.
The AAM, OAM, and HAM by ESMGFZ in Table 1 are generated by the Earth-System-Modelling group GFZ Section. 1.3 and is available from their repository, http://rz-vm115.gfz-potsdam.de:8080/repository.
The AAM based on NCEP reanalysis atmosphere and the OAM computed from ECCO model driven by NCEP atmosphere can be downloaded from Paris Observatory website, https://hpiers.obspm.fr/eop-pc/index.php?index=excitactive&lang=en.
The AAM based on JRA-55 are computed by RY. The AAM data is available from zenodo, https://doi.org/https://doi.org/10.5281/zenodo.7523914.
The program to calculate the AAM based on the JRA-55 data is uploaded to GitHub, https://doi.org/https://doi.org/10.5281/zenodo.7703445.

Declarations

Competing interests
The authors declare that they have no competing interests.

Author details
[1]Department of Natural History Sciences, Graduate School of Science, Hokkaido University, Sapporo, Japan. [2]Department of Earth and Planetary Sciences, Faculty of Science, Hokkaido University, Sapporo, Japan. [3]Arctic Research Center, Hokkaido University, Sapporo, Japan.

Received: 7 August 2023 Accepted: 8 December 2023
Published online: 02 January 2024

References
Anstey JA, Banyard TP, Butchart N, Coy L, Newman PA, Osprey S, Wright CJ (2021) Prospect of increased disruption to the QBO in a changing climate. Geophys Res Lett 48:e2021GL093058. https://doi.org/10.1029/2021GL093058
Aoyama Y, Naito I (2001) Atmospheric excitation of the Chandler wobble, 1983–1998. J Geophys Res Solid Earth 106(B5):8941–8954. https://doi.org/10.1029/2000JB900460
Aoyama Y, Naito I, Iwabuchi T, Yamazaki N (2003) Atmospheric quasi-14 month fluctuation and excitation of the Chandler wobble. Earth Planets Space 55(12):e25–e28. https://doi.org/10.1186/BF03352480
Baldwin MP, Gray LJ, Dunkerton TJ, Hamilton K, Haynes PH, Randel WJ, Holton JR, Alexander MJ, Hirota I, Horinouchi T, Jones DBA, Kinnersley JS, Marquardt C, Sato K, Takahashi M (2001) The quasi-biennial oscillation. Rev Geophys 39(2):179–229. https://doi.org/10.1029/1999RG000073
Barnes RTH, Hide R, White AA, Wilson CA (1983) Atmospheric angular momentum fluctuations, length-of-day changes and polar motion. Proc R Soc Lond A 387:31–73. https://doi.org/10.1098/rspa.1983.0050
Benjamin D, Wahr J, Ray RD, Egbert GD, Desai SD (2006) Constraints on mantle anelasticity from geodetic observations, and implications for the J2 anomaly. Geophys J Int 165:3–16. https://doi.org/10.1111/j.1365-246X.2006.02915.x
Bizouard C, Lambert S, Gattano C, Becker O, Richard JY (2019) The IERS EOP 14C04 solution for Earth orientation parameters consistent with ITRF 2014. J Geodesy 93:621–633. https://doi.org/10.1007/s00190-018-1186-3
Brzeziński A, Nastula J (2002) (2002), Oceanic excitation of the Chandler wobble. Adv Space Res 30(2):195–200. https://doi.org/10.1016/S0273-1177(02)00284-3
Chao BF (1985) On the Excitation of the Earth's polar motion. Geophys Res Lett 12(8):526–529. https://doi.org/10.1029/GL012i008p00526
Chao BF (1989) Length-of-day variations caused by El Niño-southern oscillation and quasi-biennial oscillation. Science 243:4893. https://doi.org/10.1126/science.243.4893.923
Chao BF, Chung WY (2012) Amplitude and phase variations of Earth's Chandler wobble under continual excitation. J Geodyn 62:35–39. https://doi.org/10.1016/j.jog.2011.11.009
Chen JL, Wilson CR, Ries JC, Tapley BD (2013) Rapid ice melting drives Earth's pole to the east. Geophys Res Lett 40:2625–2630. https://doi.org/10.1002/grl.50552
Dahlen FA (1973) A correction to the excitation of the Chandler wobble by earthquakes. Geophys J R Astron Soc 32:203–217. https://doi.org/10.1111/j.1365-246X.1973.tb06527.x
Dill R (2008) Hydrological model LSDM for operational Earth rotation and gravity field variations. Deutsches GeoForschungsZentrum GFZ, Potsdam
Dobslaw H, Dill R, Grötzsch A, Brzeziński A, Thomas M (2010) Seasonal polar motion excitation from numerical models of atmosphere, ocean, and continental hydrosphere. J Geophys Res 115:B10406. https://doi.org/10.1029/2009JB007127
Eubanks T, Steppe J, Dickey J, Rosen R, Salstein D (1988) Causes of rapid motions of the Earth's pole. Nature 334:115–119. https://doi.org/10.1038/334115a0
Furuya M, Hamano Y, Naito I (1996) Quasi-periodic wind signal as a possible excitation of Chandler wobble. J Geophys Res 101(B11):25537–25546. https://doi.org/10.1029/96JB02650
Furuya M, Chao BF (1996) Estimation of period and Q of the Chandler wobble. Geophys J Int 127(3):693–702. https://doi.org/10.1111/j.1365-246X.1996.tb04047.x
Furuya M, Hamano Y, Naito I (1997) Importance of wind for the excitation of Chandler wobble as inferred from wobble domain analysis. J Phys Earth 45(3):177–188. https://doi.org/10.4294/jpe1952.45.177
Gross RS (2000) The excitation of the Chandler wobble. Geophys Res Lett 27(15):2329–2332. https://doi.org/10.1029/2000GL011450
Gross RS, Fukumori I, Menemenlis D (2003) Atmospheric and oceanic excitation of the Earth's wobbles during 1980–2000. J Geophys Res 108(B8):2370. https://doi.org/10.1029/2002JB002143
Gross RS (2015) Earth rotation variations—long period. In: Schubert G (ed) Treatise in Geophysics, 2nd edn. Amsterdam, Elsevier
Kobayashi S, Ota Y, Harada Y, Ebita A, Moriya M, Onoda H, Onogi K, Kamahori H, Kobayashi C, Endo H, Miyaoka K, Takahashi K (2015) The JRA-55 reanalysis: general specifications and basic characteristics. J Meteorol Soc Jpn 93:5–48. https://doi.org/10.2151/jmsj.2015-001
Malkin Z, Miller N (2010) Chandler wobble: two more phase jumps revealed. Earth Planets Space 62:943–947. https://doi.org/10.5047/eps.2010.11.002
Munk WH, MacDonald GJF (1960) The rotation of the Earth: a geophysical discussion. Cambridge University Press, New York
Nastula J, Gross R (2015) Chandler wobble parameters from SLR and GRACE. J Geophys Res Solid Earth 120:4474–4483. https://doi.org/10.1002/2014JB011825
Newman PA, Coy L, Pawson S, Lait LR (2016) The anomalous change in the QBO in 2015–2016. Geophys Res Lett 43:8791–8797. https://doi.org/10.1002/2016GL070373
Okubo S (1982) Is the Chandler period variable? Geophys J R Astron Soc 71(3):629–646. https://doi.org/10.1111/j.1365-246X.1982.tb02789.x
Osprey SM, Butchart N, Knight JR, Scaife AA, Hamilton K, Anstey JA, Schenzinger V, Zhang C (2016) An unexpected disruption of the atmospheric quasi-biennial oscillation. Science 353:6306. https://doi.org/10.1126/science.aah4156
Ponte R, Stammer D, Marshall J (1998) Oceanic signals in observed motions of the Earth's pole of rotation. Nature 391:476–479. https://doi.org/10.1038/35126
Plag HP (1997) Chandler wobble and pole tide in relation to interannual atmosphere-ocean dynamics. In: Wilhelm H, Zürn W, Wenzel H-G (eds) Tidal Phenomena Lecture Notes in Earth Sciences. Springer, Heidelberg, pp 183–218
Seitz F, Schmidt M (2005) Atmospheric and oceanic contributions to Chandler wobble excitation determined by wavelet filtering. J Geophys Res 110:B11406. https://doi.org/10.1029/2005JB003826
Seitz F, Kirschner S, Neubersch D (2012) Determination of the Earth's pole tide Love number k2 from observations of polar motion using an adaptive Kalman filter approach. J Geophys Res Solid Earth 117:B09403. https://doi.org/10.1029/2012JB009296
Smith ML, Dahlen FA (1981) The period and Q of the Chandler wobble. Geophys J R Astron Soc 64:223–281. https://doi.org/10.1111/j.1365-246X.1981.tb02667.x

Vondrák J, Ron C (2005) The great Chandler wobble change in 1923–1940 re-visited. In: Plag HP, Chao BF, Gross RS, van Dam T (eds) Forcing of Polar Motion in the Chandler Frequency Band: A Contribution to Understanding Interannual Climate Change. Cahiers du Centre Européen de Géodynamique et de Séismologie, Luxembourg, pp 39–42
Wilson CR, Vicente RO (1990) Maximum likelihood estimates of polar motion parameters. In: McCarthy DD, Carter WE (eds) Variations in Earth Rotation, Geophysical Monograph Series. American Geophysical Union, Washington, pp 151–155
Wilson CR (1985) Discrete polar motion equations. Geophys J R Astron Soc 80:551–554. https://doi.org/10.1111/j.1365-246X.1985.tb05109.x
Zotov L, Bizouard C, Shum CK, Zhang C, Sidorenkov N, Yushkin V (2022) Analysis of Earth's polar motion and length of day trends in comparison with estimates using second degree stokes coefficients from satellite gravimetry. Adv Space Res 69(1):308–318. https://doi.org/10.1016/j.asr.2021.09.010

Publisher's Note